Modeling of Nonisothermal Film Blowing Process for Non-Newtonian Fluids by Using Variational Principles

Roman Kolarik, Martin Zatloukal

Centre of Polymer Systems, Polymer Centre, Tomas Bata University in Zlin, nam. T. G. Masaryka 5555, 760 01 Zlin, Czech Republic

Received 4 August 2010; accepted 12 February 2011
DOI 10.1002/app.34392
Published online 29 June 2011 in Wiley Online Library (wileyonlinelibrary.com).

ABSTRACT: In this work, nonisothermal film blowing process analysis for non-Newtonian polymer melts has been performed theoretically by using minimum energy approach and the obtained predictions were compared with both, theoretical and experimental data (internal bubble pressure, take-up force, bubble shape, velocity and temperature profiles) taken from the open literature. For this purpose, recently proposed generalized Newtonian model depending on three principal invariants of the deformation rate tensor, D, and its absolute defined as $\sqrt{D \cdot D}$ has been used. It has been found that film blowing model predictions are in very good agreement with the corresponding experimental data. © 2011 Wiley Periodicals, Inc. J Appl Polym Sci 122: 2807–2820, 2011

Key words: extrusion; films; mathematical modeling; non-newtonian fluids; numerical analysis; polymers; polymer processing; rheology

INTRODUCTION

The film blowing process is an important polymer processing operation which is widely used for thin polymer films production.[1–29] At the beginning of the process, polymer pellets go through the extruder hopper to the thread of the screw, where pellets are transported, homogenized, compressed, and melted. Then, the polymer melt is extruded at a constant flow rate through an annular die to a continuous tube, as can be seen in Figure 1, which describes the most often used film blowing line type, the nip rolls situated on the top of the line. The continuous tube is stretched in two directions: the axial drawing (machine direction) by the nip rolls and the circumferential drawing (transverse direction) by the internal air pressure. Simultaneously, the bubble is cooled by an air ring (with/without internal bubble cooling system IBC) situated around the bubble level with the die exit. Then, above the freezeline height, the bubble is in a solid state, with the final mechanical and optical properties. Calibration bubble cage is usually used to stabilize the system. The dimensions of the bubble are defined by the terms blow-up ratio, BUR, which is the ratio of the final bubble diameter at the freezeline height to the bubble diameter at the die exit, and the take-up ratio, TUR, which is the ratio of the film velocity above the freezeline to the melt velocity through die exit. Above the calibration cage, the bubble is folded between two table flaps and drawn by the nip rolls to a wind-up roll. These biaxially oriented films of a small thickness are used in commodity applications, such as food wrapping and carrier bags in food processing, medical films, scientific balloons, garbage bags, and waste land fill liners in the waste industry.[3]

The relationships between the machine design, processing parameters, material and the extensional stresses within the extending bubble are still not fully understood although they have been investigated by many researchers from the late 1930's.[1–14] The most popular way to optimize the film blowing process is modeling. The first film blowing model was developed by Pearson and Petrie[20,22] for isothermal process and Newtonian fluid where the film is assumed to be a thin shell in tension in the axial and circumferential directions. This model became the basis of the most subsequent film blowing models.[15–17,24,26,30–36] However, numerical instabilities,[26,29] inability to describe the full range of the bubble shapes[27] and existence of anomalous predictions[37,38] were identified in the open literature if one tried to solve the Pearson-Petrie

Correspondence to: M. Zatloukal (mzatloukal@ft.utb.cz).
Contract grant sponsor: GA CR; contract grant number: P108/10/1325.
Contract grant sponsor: MSMT (project Centre of Polymer Systems); contract grant number: CZ.1.05/2.1.00/03.0111.

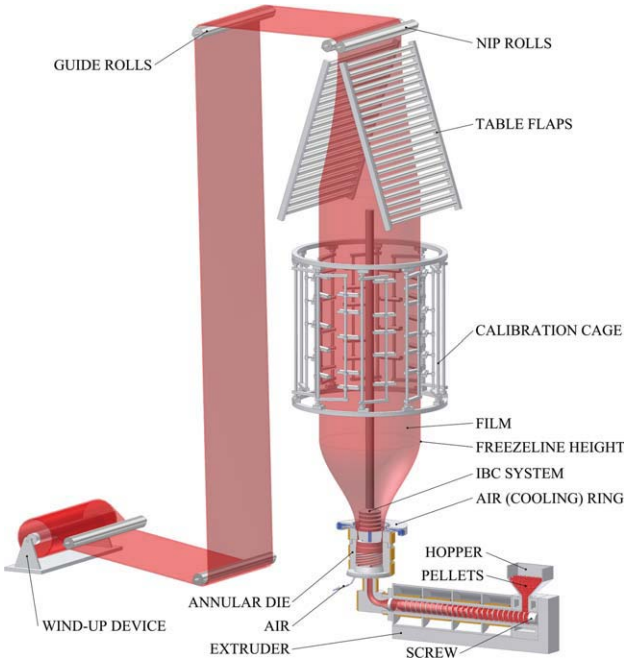

Figure 1 The film blowing line. [Color figure can be viewed in the online issue, which is available at wiley onlinelibrary.com.]

equations with particular constitutive equations. It has been recently found that these problems can be overcome by the use of the Zatloukal-Vlcek model,[30–36] which describes the formation of the bubble, because of the internal bubble pressure and the take-up force, in such a way that the resulting bubble satisfies the minimum energy requirements.

The main aim in this work is to investigate predicting capabilities of the Zatloukal-Vlcek model if nonisothermal conditions and non-Newtonian fluid behavior are taken into account. The studied model behavior will be compared with Tas's Ph.D. thesis experimental data[18] and predictions of the following two different Pearson and Petrie based models: Sarafrazi and Sharif model[16] (extended Pom-Pom constitutive equation is used; a variable heat transfer coefficient and stress induced crystallization is taken into account) and Beaulne and Mitsoulis model[15] (integral constitutive equation of the K-BKZ type is utilized; constant heat transfer coefficient and no crystallization effects are assumed).

MATHEMATICAL MODELING

It has been shown by Zatloukal and Vlcek[31] that the bubble during blowing can be viewed as a bended elastic membrane due to the load p and the take-up force F, where the line element of the membrane after loading can be simplified as $\sqrt{1+(y')^2}dx \approx \left[1+\frac{1}{2}(y')^2\right]dx$ (see Fig. 2). In such a case, the membrane potential energy can be expressed by the following form:

$$E_p = \frac{F}{2}\int_0^L (y')^2 dx - p\int_0^L y dx \tag{1}$$

which takes into account two basic contributions to the potential energy: elastic strain energy increase and negative work done by the applied load. Having the bubble volume, $V = \pi\int_0^L y^2 dx$, as the main geometrical constrain, the equation for the bubble shape, y, can be derived through minimization of the potential energy functional, I, in the following form:

$$I = \left[\frac{1}{2}F(y')^2 - py\right] + \lambda_1(\pi y^2) \tag{2}$$

i.e., $I = f(x, y, y')$ where λ_1 is the Lagrange multiplier. The functional I is minimized if the following equation is satisfied:

$$\frac{\partial I}{\partial y} - \frac{\partial}{\partial x}\frac{\partial I}{\partial y'} = 0 \tag{3}$$

Equations (2) and (3) yield the following differential equation:

$$Fy'' - \frac{1}{J}y + p = 0 \tag{4}$$

Where J is the compliance of the membrane defined as positive constant taking the following form:

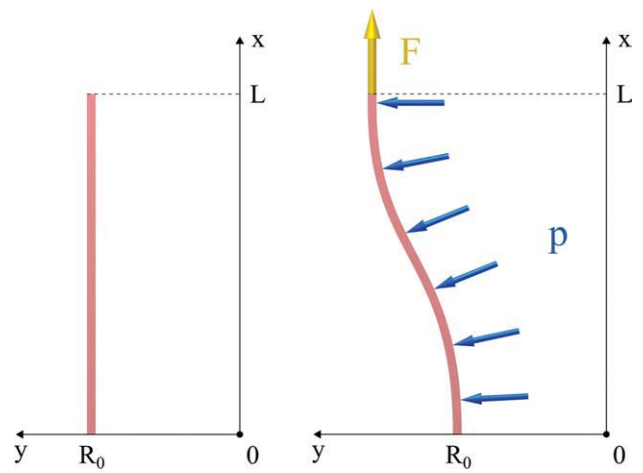

Figure 2 Membrane before deformation (left), membrane after deformation (right). [Color figure can be viewed in the online issue, which is available at wileyonlinelibrary.com.]

TABLE I
Relationship Between A and φ Functions

Equation number	A	φ
(1)	1	0
(2)	$0 < A < 1$	$arctg\left(\frac{\sqrt{1-A^2}}{A}\right)$
(3)	0	π/2
(4)	$-1 < A < 0$	$\pi + arctg\left(\frac{\sqrt{1-A^2}}{A}\right)$
(5)	−1	π

$$J = \frac{1}{2\pi\lambda_1} \tag{5}$$

Let us use the following boundary conditions for the bubble shape:

$$\frac{\partial y(x=L)}{\partial x} = 0, \quad y(x=0) = R_0 \tag{6}$$

and

$$y(x=L) = R_0\mathrm{BUR} = R_2 \tag{7}$$

where R_0 is the extrusion die radius, L the freezeline height and R_2 is the bubble radius at the freezeline, i.e., $x = L$. Since above the freezing line there is no deformation, it can be assumed that $y(x > L) = const. = y(x = L)$. It is not difficult to show (see Ref. [31] for detailed derivation) that the solution of eq. (4), considering the aforementioned boundary conditions, takes the following form:

$$y = (R_0 - pJ)\cos\left(\frac{x\varphi}{L}\right) - \alpha'(pJ - \mathrm{BURR}_0)\sin\left(\frac{x\varphi}{L}\right) + pJ \tag{8}$$

where force F is given by the following expression:

$$F = -\frac{L^2}{J\varphi^2} \tag{9}$$

Here α' and A are given below and the value of $\varphi(A)$ is calculated according to Table I:

$$\alpha' = \sqrt{\frac{2pJ - R_0 - \mathrm{BUR}\ R_0}{pJ - \mathrm{BUR}\ R_0}\left|\frac{R_0(\mathrm{BUR} - 1)}{pJ - \mathrm{BUR}\ R_0}\right|} \tag{10}$$

$$A = \frac{pJ - R_0}{pJ - \mathrm{BUR}\ R_0} \tag{11}$$

The total number of parameters needed to describe the bubble shape is equal to four (pJ, L, R_0, BUR). Just note that pJ/R_0 (dimensionless form of pJ) determines the total deformation (curvature) of the bubble which varies between 0 and $Ro*(1+\mathrm{BUR})/2$ for the bubbles without the neck.[31]

According to,[31] the internal bubble pressure and the take-up force for a 3D bubble can be directly calculated from parameters of the proposed model and the force balance by taking the 3D nature of a real bubble into account through following equations:

$$\Delta p = \frac{pL}{2\pi\int_0^L y\sqrt{1 + (y')^2 dx}} \tag{12}$$

$$F_{\mathrm{total}} = |F| \tag{13}$$

where the term $2\pi\int_0^L y\sqrt{1 + (y')^2 dx}$ in eq. (12) means the bubble surface and the term pL is the force acting in the thickness direction of the bubble, $F_{\mathrm{thickness}}$. Eq. (12) represents the calculation of the internal bubble pressure in such a way that the bubble is represented by an equivalent cylinder, which has the same surface as the real bubble. Force F in eq. (13) is defined by eq. (9).

Nonisothermal film blowing with non-Newtonian fluid

In this section, the assumptions about the static (not moving) and elastic only bubble having constant thickness will be relaxed. It is done here by considering an additional set of equations, which are summarized below.

Continuity equation:

$$Q = 2\pi y(x)h(x)v(x) \tag{14}$$

where Q is the volume flow rate, $y(x)$, the radius of the bubble, $h(x)$, the thickness of the film and $v(x)$ is the film velocity, all as functions of the distance from the die x.

Constitutive equation (generalized Newtonian fluid recently proposed in[39]):

$$\tau = 2\eta\left(I_{|D|}, II_D, III_D\right)D \tag{15}$$

where τ means the extra stress tensor, D represents the deformation rate tensor and η stands for the viscosity, which is not constant (as in the case of standard Newtonian law), but it is allowed to vary with the first invariant of the absolute value of deformation rate tensor $I_{|D|} = tr(|D|)$, (where $|D|$ is defined as the square root of D^2) as well as on the second $II_D = 2tr\left(D^2\right)$, and third, $III_D = \det(D)$, invariants of D according to eq. (16)

$$\eta\left(I_{|D|}, II_D, III_D\right) = \eta(II_D)^{f\left(I_{|D|}, II_D, III_D\right)} \tag{16}$$

where $\eta(II_D)$ is given by the well known Carreau-Yasuda model, eq. (17) and $f\left(I_{|D|}, II_D, III_D\right)$ is given by eq. (18).

$$\eta(II_D) = \frac{\eta_0 a_T}{\left[1 + \left(\lambda a_T \sqrt{II_D}\right)^a\right]^{\left(\frac{1-n}{a}\right)}} \quad (17)$$

$$f(I_{|D|}, II_D, III_D) = \left\{ \tanh\left[\alpha a_T \left(1 + \frac{1}{4(\sqrt{3})^3}\right)^{-\psi} \left(\left|1 + \frac{III_D}{II_D^{3/2}}\right|\right)^{\psi} \frac{\sqrt[3]{4|III_D|} + I_{|D|}}{3} + \beta\right] \frac{1}{\tanh(\beta)}\right\}^{\zeta} \quad (18)$$

Here η_0, λ, a, n, α, ψ, β, ζ are adjustable parameters and a_T is temperature shift factor defined by the Arrhenius equation:

$$a_T = \exp\left[\frac{E_a}{R}\left(\frac{1}{273.15 + T} - \frac{1}{273.15 + T_r}\right)\right] \quad (19)$$

where E_a is the activation energy, R is the universal gas constant, T_r is the reference temperature and T is local bubble temperature. This recently proposed constitutive equation in[39] has been chosen for the film blowing modeling because it has high flexibility to represent the strain rate dependent steady shear and uniaxial extensional viscosities for linear and branched polyolefines as well as it provides correct behavior in steady planar/equibiaxial extensional viscosity. Moreover, the model allows independent strain hardening level control for planar/equibiaxial extensional viscosity with respect to uniaxial extensional viscosity through parameter ψ.[39]

It is not difficult to show that the equation of continuity ($Q = Sv_f$) together with the generalized Newtonian model (applied for the machine direction stress $\tau_{xx} = 2\overline{\eta}\overline{\dot{\varepsilon}_1}$) yields the following expression for the internal force ($F_N = \tau_{xx}S$) at the freezeline in the machine direction:

$$F_N = 2\overline{\eta}\overline{\dot{\varepsilon}_1}\frac{Q}{v_f} \quad (20)$$

where $\overline{\eta}$ and $\overline{\dot{\varepsilon}_1}$ represent the mean values of the melt viscosity ($\overline{\eta} = \frac{1}{L}\int_0^L \eta dx$) and the extensional rate ($\overline{\dot{\varepsilon}_1} = \frac{1}{L}\int_0^L \dot{\varepsilon} dx$), respectively, for the whole bubble, Q, the volume flow rate, v_f, the velocity of the film at the freezeline. The equation for bubble compliance J can be obtained by solving eqs. (9), (13), and (20) in the following form:

$$J = \frac{L^2 v_f}{2\varphi^2 \overline{\eta}\overline{\dot{\varepsilon}_1} Q} \quad (21)$$

Energy equation

With the aim to take nonisothermal conditions into account, cross sectionally averaged energy equation taken from,[40] has been considered:

$$\rho C_p \frac{dT}{dx} = -\frac{2\pi y \rho}{\dot{m}}[HTC(T - T_{\text{air}}) + \sigma_B \bar{\varepsilon}(T^4 - T_{\text{air}}^4)] + \tau : \nabla v + \rho \Delta H_f \frac{d\phi}{dx} \quad (22)$$

where C_p stands for the specific heat capacity, ρ is the polymer density, y means the local bubble radius, $\dot{m}$ is the mass flow rate, HTC represents the heat transfer coefficient, T is the bubble temperature, T_{air} means the air temperature used for the bubble cooling, σ_B stands for the Stefan-Boltzmann constant, $\bar{\varepsilon}$ represents the emissivity, τ is the extra stress tensor, ∇v means velocity gradient tensor, ΔH_f indicates the heat of crystallization per unit mass and ϕ is the average absolute crystallinity degree of the system at the axial position, x.

To reduce the problem complexity, the axial conduction, dissipation, radiation effects, and crystallization are neglected. For such simplifying assumptions, eq. (22) is reduced in the following, the simplest version of the cross sectionally averaged energy equation:

$$\dot{m} C_p \frac{dT}{dx} = 2\pi y[HTC(T - T_{\text{air}})] \quad (23)$$

where the local bubble radius y is given by eq. (8). It should be mentioned that neglecting several terms in eq. (22) for the energy equation (especially crystallization) may be the reason for the poor predicted of the temperature profile along the bubble in the range of the polymer freezing point. The eq. (23) applied for the whole part of the bubble takes the following form:

$$\int_{T_{\text{die}}}^{T_{\text{solid}}} \frac{\dot{m} C_p}{HTC(T - T_{\text{air}})} dT = 2\pi \int_0^L y dx \quad (24)$$

where T_{die} and T_{solid} represents the temperature of the melt at the die exit and solidification temperature of the polymer, respectively. After integration from die temperature, T_{die}, up to freezeline temperature, T_{solid}, we can obtain equation defining the relationship between freezeline height, L, and heat transfer coefficient, HTC, which takes the following simple analytical expression:

$$L = -\frac{1}{2}\dot{m} C_p \ln\left(-\frac{(T_{\text{die}} - T_{\text{air}})}{(-T_{\text{solid}} + T_{\text{air}})}\right) \frac{\varphi}{\pi HTC(\alpha p J - \alpha \text{BURR}_0 - \sin(\varphi) R_0 - pJ\varphi + \sin(\varphi) pJ - \alpha \cos(\varphi) pJ + \alpha \cos(\varphi) \text{BURR}_0)} \quad (25)$$

With the aim to get equations for the temperature profile along the bubble, it is necessary to apply the eq. (23) for any arbitrary point at the bubble, i.e., in the following way:

$$\int_{T_{die}}^{T} \frac{\dot{m}C_p}{HTC(T-T_{air})}dT = 2\pi \int_0^x y dx \tag{26}$$

After the integration of eq. (26), the temperature profile takes the following analytical expression:

$$T = T_{air} + (T_{die} - T_{air}) \exp\left\{-\frac{2\pi LHTC}{\dot{m}C_p\varphi}\left(-\alpha[R_0\mathrm{BUR} - pJ] \times \left[\cos\left(\frac{x\varphi}{L}\right) - 1\right] + \sin\left(\frac{x\varphi}{L}\right)[R_0 - pJ] + pJ\varphi\frac{x}{L}\right)\right\} \tag{27}$$

Velocity profile calculation

With the aim to calculate the velocity profile and the film thickness in the nonisothermal film blowing process, the force balance in vertical direction (gravity and upward force due to the airflow are neglected) proposed by Pearson and Petrie is considered in the following form:

$$\frac{2\pi y h \sigma_{11}}{\sqrt{1+(y')^2}} = F - \pi\Delta p\left(R_0^2\mathrm{BUR}^2 - y^2\right) \tag{28}$$

where σ_{11} is the total stress in the machine direction and F and Δp are defined by eqs. (9), (13), and (12). The deformation rate tensor in the bubble forming region takes the following form:

$$D = \begin{pmatrix} \dot{\varepsilon}_1 & 0 & 0 \\ 0 & \dot{\varepsilon}_2 & 0 \\ 0 & 0 & \dot{\varepsilon}_3 \end{pmatrix} = \begin{pmatrix} \frac{dv}{dx} & 0 & 0 \\ 0 & \frac{v}{h}\frac{dh}{dx} & 0 \\ 0 & 0 & \frac{v}{y}y' \end{pmatrix} \tag{29}$$

where v and h is bubble velocity and thickness, respectively. Assuming that $h \ll y$, then

$$\sigma_{11} = \tau_{11} - \tau_{22} \tag{30}$$

By combination of eqs. (15), (29), (30), the σ_{11} takes the following form:

$$\sigma_{11} = 2\eta\left(2\frac{dv}{dx} + \frac{v}{y}y'\right) \tag{31}$$

After substituting eq. (31) into eq. (28), the equation for the bubble velocity in the following form can be obtained.

$$v = v_d \exp \times\left(\int_0^L \left\{\frac{\sqrt{1+(y')^2}\left[F - \pi\Delta p\left(R_0^2\mathrm{BUR}^2 - y^2\right)\right]}{4Q\eta} - \frac{1}{2y}y'\right\}dx\right) \tag{32}$$

where v_d is bubble velocity at the die exit. Having the velocity profile, the deformation rates and the thickness can be properly calculated along the bubble. The key film blowing variables are depicted in Figure 3.

MODELING VERSUS EXPERIMENTAL DATA

In this part, the above described film blowing model will be tested by using experimental data taken from the Tas's Ph.D. thesis.[18] Moreover, theoretical predictions will be compared with two different film blowing models[15–17] (those predictions will be taken from the literature), which has already been utilized for the same experimental data set.

Material definition

In this work, LDPE L8 taken from Tas's Ph.D. thesis[18] is considered. Material characteristics together

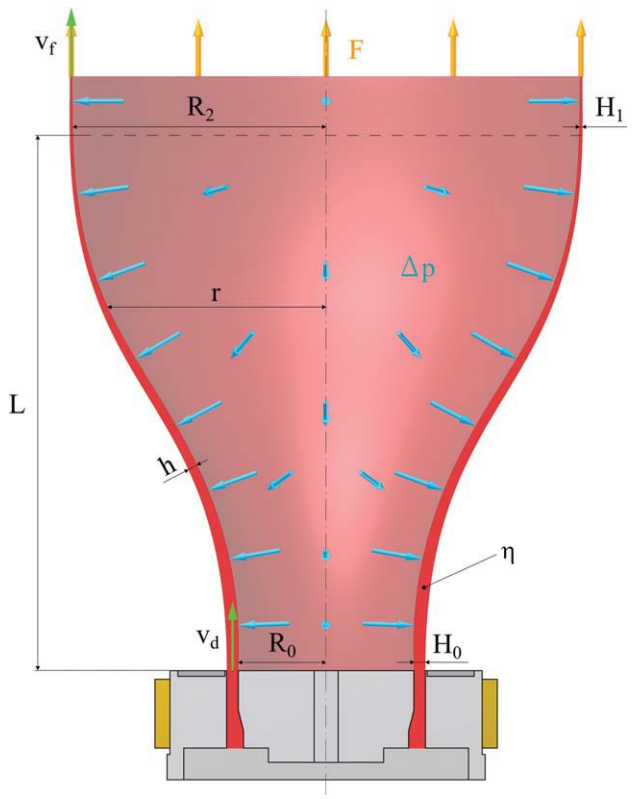

Figure 3 Film blowing variables. [Color figure can be viewed in the online issue, which is available at wiley onlinelibrary.com.]

TABLE II
Characteristics of the L8 Stamylan LDPE Used in the Experiments by Tas[18]

LDPE material	Grade (Stamylan LD)	Melt Index (dg.min^{-1})	Molecular weight averages			Density (kg m^{-3})	Crystallization temperature T_c (°C)
			M_n (g mol^{-1})	M_w (g mol^{-1})	M_z (g mol^{-1})		
L8	2008XC43	8	13,000	155,000	780,000	920	98.6

with corresponding viscoelastic Phan-Thien-Tanner (PTT) model parameters are provided in Tables II and III. It should be mentioned that predictions of the PTT model[41] for steady state shear and steady uniaxial extensional viscosities have been used as the measurements for LDPE L8 to obtain all adjustable parameters of the proposed model [eqs. (16–18)], which is utilized here as the constitutive equation. This procedure has been chosen due to the fact that steady state rheological data for tested LDPE L8 is not available in Tas's Ph.D. thesis.

In Figure 4, it is clearly visible that the used generalized Newtonian model has very good capabilities to describe steady shear and steady uniaxial extensional viscosities for the Tas's LDPE L8 sample, which justifies its utilization in the film blowing modeling. The generalized Newtonian model parameters are provided in Table IV and the parameter ψ has been chosen to be 20 as suggested in.[39]

Numerical scheme

To determine the heat transfer coefficients for the Tas's film blowing experimental data, first, the eq. (8) has been used to fit the Tas's bubble shapes to obtain all model parameters (R_0, L, BUR and pJ). In the second step, the heat transfer coefficient HTC for each specific condition has been determined by using eq. (25).

On the basis of the input parameters (see numerical scheme in Fig. 5) and guess values for pJ, Δp, $\overline{I_{|D|}}$, $\overline{II_D}$, and $\overline{III_D}$, so called average bubble viscosity $\overline{\eta}$ can be determined according to eq. (33)

$$\overline{\eta} = \left\{ \frac{\eta_0 \overline{a_T}}{\left[1 + \left(\lambda \overline{a_T} \sqrt{\overline{II_D}}\right)^a\right]^{\left(\frac{1-n}{a}\right)}} \right\} \left\{ \tanh\left[\alpha \overline{a_T} \left(1 + \frac{1}{4(\sqrt{3})^3}\right)^{-\psi} \left(\left| 1 + \frac{\overline{III_D}}{II_D^{3/2}} \right| \right)^{\psi} \frac{\sqrt[3]{4\left|\overline{III_D}\right|} + \overline{I_{|D|}}}{3} + \beta \right]^{\frac{1}{\tanh(\beta)}} \right\}^{\zeta} \tag{33}$$

where $\overline{I_{|D|}}$ is the mean value of the first invariant of the square root of D^2, $\overline{II_D}$, and $\overline{III_D}$ represent the mean value of the second and third invariants of deformation rate tensor, respectively, and $\overline{a_T}$ is the average temperature shift factor [eq. (33)]:

$$\overline{I_{|D|}} = \sqrt{\overline{\dot{\varepsilon}_1^2}} + \sqrt{\overline{\dot{\varepsilon}_2^2}} + \sqrt{\overline{\dot{\varepsilon}_3^2}}$$
$$\overline{II_D} = 2\left(\overline{\dot{\varepsilon}_1^2} + \overline{\dot{\varepsilon}_2^2} + \overline{\dot{\varepsilon}_3^2}\right) \tag{34}$$

$$\overline{III_D} = \overline{\dot{\varepsilon}_1 \dot{\varepsilon}_2 \dot{\varepsilon}_3} \tag{35}$$

$$\overline{a_T} = \exp\left[\frac{E_a}{R}\left(\frac{1}{273.15 + T_s} - \frac{1}{273.15 + T_r}\right)\right] \tag{36}$$

Here, the average bubble temperature T_S and mean values of the deformation rate components $\overline{\dot{\varepsilon}_1}, \overline{\dot{\varepsilon}_2}, \overline{\dot{\varepsilon}_3}$ are defined as follows

$$T_S = \frac{T_{\text{die}} + T_{\text{solid}}}{2} \tag{37}$$

$$\overline{\dot{\varepsilon}_1} = \frac{1}{L}\int_0^L \dot{\varepsilon}_1 dx \tag{38}$$

$$\overline{\dot{\varepsilon}_2} = \frac{\overline{v}\,\overline{h} - H_0}{\overline{h}\,L} \tag{39}$$

TABLE III
Discrete Relaxation Time Spectra Together With Nonlinear PTT[41] Model Parameters ξ and ε at 190°C for L8 Stamylan LDPE Sample

L8 ($\xi = 0.13$, $\varepsilon = 0.05$)	
λ_i (s)	G_i (Pa)
4.28×10^{-5}	2.17×10^{5}
2.07×10^{-4}	9.18×10^{4}
1.34×10^{-3}	5.75×10^{4}
9.02×10^{-3}	2.43×10^{4}
5.69×10^{-2}	8.91×10^{3}
3.53×10^{-1}	2.34×10^{3}
1.82×10^{0}	3.21×10^{2}
9.94×10^{0}	1.24×10^{1}

Data are taken from Tas's Ph.D. thesis.[18]

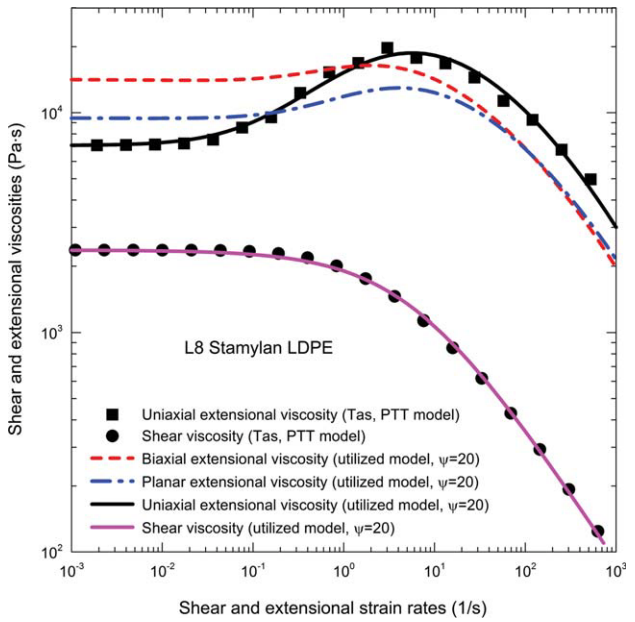

Figure 4 Comparison between the generalized Newtonian model fit (solid lines)[39] and PTT model predictions (symbols) characterizing L8 Stamylan LDPE material according to Tas's Ph.D. thesis.[18] [Color figure can be viewed in the online issue, which is available at wileyonlinelibrary.com.]

$$\overline{\dot{\varepsilon}_3} = -\left(\overline{\dot{\varepsilon}_1} + \overline{\dot{\varepsilon}_2}\right) \tag{40}$$

where L is freezeline height, H_0 is bubble thickness at the die, $\overline{v}$ and $\overline{h}$ is mean value of bubble velocity and thickness along the bubble, respectively, which are defined bellow:

$$\overline{v} = \frac{1}{L}\int_0^L v(x)dx \tag{41}$$

$$\overline{h} = \frac{1}{L}\int_0^L h(x)dx \tag{42}$$

It is well known that during the film blowing process, the melt viscosity is changing dramatically between the extrusion die exit and freezeline height. To take such strong temperature dependence of the viscosity during velocity calculation of the film [by using eq. (32)] into account, the following expression for the viscosity η has been proposed and used:

$$\eta = \overline{\eta}\, a_{T,\text{Bubble}} \tag{43}$$

where $a_{T,\text{Bubble}}$ is the normalized bubble temperature shift factor defined as:

$$a_{T,\text{Bubble}} = \frac{a_T}{a_{TS}} \tag{44}$$

where a_{TS} represents the mean value of the Arrhenius temperature shift factor a_T [see eq. (19)], which is given as follows:

$$a_{TS} = \frac{1}{L}\int_0^L a_T dx \tag{45}$$

The velocity profile is calculated by the help of eq. (32) where the take-up force F is varied until the calculated film velocity at the freezeline height reached the desirable value (according to defined TUR). For the obtained velocity profile, the average bubble viscosity $\overline{\eta}$ is upgraded (based on the new values of three deformation rate tensor invariants $\overline{I_{|D|}}$, $\overline{II_D}$, and $\overline{III_D}$) and the velocity calculation is repeated again until the average bubble viscosity $\overline{\eta}$

TABLE IV
Film Blowing Model Parameters for Tas's Experiments No. 23 and 29 and L8 Stamylan LDPE Material

Input parameters for the Zatloukal-Vlcek film blowing model								
Exp.	BUR (−)	L (m)	pJ (m)	Δp (Pa)	R_0 (m)	H_0 (m)	TUR (−)	$\dot{m}$ (kg s^{-1})
23	2.273	0.13365	0.027605	85	0.0178	0.0022	21.5083	0.00100
29	2.749	0.13882	0.029818	70	0.0178	0.0022	19.4437	0.00100

Parameters of the generalized Newtonian constitutive equation ($\psi = 20$)						
η_0 (Pa s)	λ (s)	a (−)	n (−)	α (s)	β (−)	ζ (−)
2,365	0.17242	0.71597	0.37108	1.10^{-5}	$9.21.10^{-7}$	0.054384

Temperature parameters						
T_{air} (°C)	T_{solid} (°C)	T_{die} (°C)	T_r (°C)	E_a (J mol^{-1})	R (J K^{-1} mol^{-1})	C_p (J kg^{-1} K^{-1})
25	92	145	190	59,000	8.314	2,300

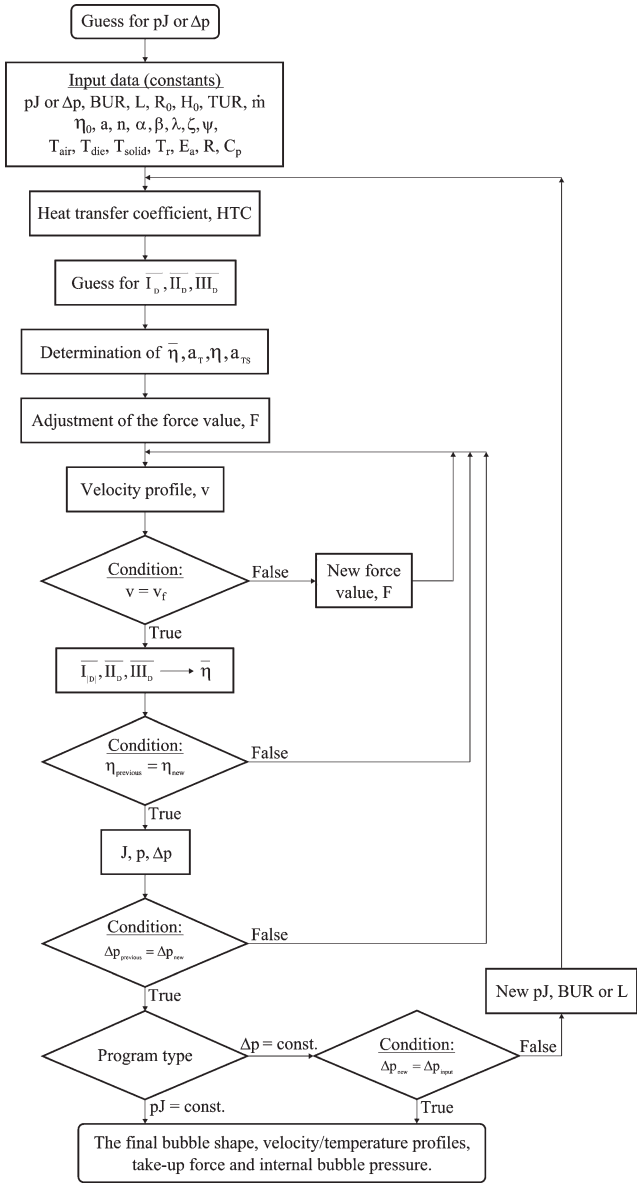

Figure 5 Iteration scheme for the proposed film blowing model.

remains unchanged for the given take-up force F and velocity profile.

In the final case, the bubble compliance J is calculated according to eq. (21). For the given pJ value (bubble curvature) the internal load is determined and consequently used for the internal bubble pressure Δp [eq. (12)] calculation. By using this new Δp value the velocity profile calculation is repeated again until the Δp becomes constant. Above described numerical scheme is summarized in Figure 5. In this way, the internal bubble pressure and take-up force can be calculated for the given bubble shape. If the internal bubble pressure is fixed, whereas the take-up force and bubble shapes (i.e., pJ), are calculated variables, the above described numerical scheme can be repeated for different values of pJ until desirable Δp is obtained.

Film blowing experiment versus model prediction

In this section, proposed model predictions for the bubble shape (Figs. 6 and 7), film velocity (Fig. 8 and 9), and temperature profiles (Figs. 10 and 11), for the processing conditions summarized in Table IV, are compared with Tas's experimental data[18] together with theoretical predictions by Sarafrazi and Sharif[16] model and Beaulne and Mitsoulis model,[15] which are based on the classical approach of Pearson and Petrie.[20]

It should be mentioned that two possible numerical schemes have been tested for the proposed model. First procedure consider that the bubble shape (i.e., pJ, BUR) is a priori known and take-up force F and internal bubble pressure Δp are unknowns parameters, whereas in the second case Δp is known and bubble shape (i.e., pJ, BUR) and F are unknown parameters (see numerical scheme in Fig. 5).

As can be clearly seen in Figures 6–11, both numerical approaches leads to very similar predictions for all investigated variables (bubble shape, velocity, and temperature) and it can be concluded that the agreement between the proposed model predictions are in very good agreement with the corresponding experimental data. Moreover, tested model predictions are comparable with the Sarafrazi and Sharif[16] model predictions (which is based on the advanced extended Pom-Pom constitutive equation; a variable heat transfer coefficient and stress induced crystallization).

Complete set of calculated variables in the proposed model for theoretical predictions depicted in Figures 6–11 are summarized in Tables V and VI. It is visible that predicted F and Δp for all tested polymers and processing conditions are in fairly good agreement with the corresponding Tas's experimental data. These predictions are comparable with Sarafrazi and Sharif[16] model predictions and even better than Beaulne and Mitsoulis model[15] behaviour, which is based on the viscoelastic integral constitutive equation of the K-BKZ type assuming constant heat transfer coefficient and no crystallization effects. Just note that for the die volume rate calculation (from the experimentally known mass flow rate), the following definition of the LDPE density taken from[18] was used:

$$\rho = \frac{1,000}{0.934 \cdot 0.001 \cdot (273.15 + T_{\mathrm{die}}) + 0.875} \qquad (46)$$

As it can be seen, the proposed approach for the film blowing modeling is comparable with the Pearson and Petrie based models for the tested polymers and processing conditions. It should be

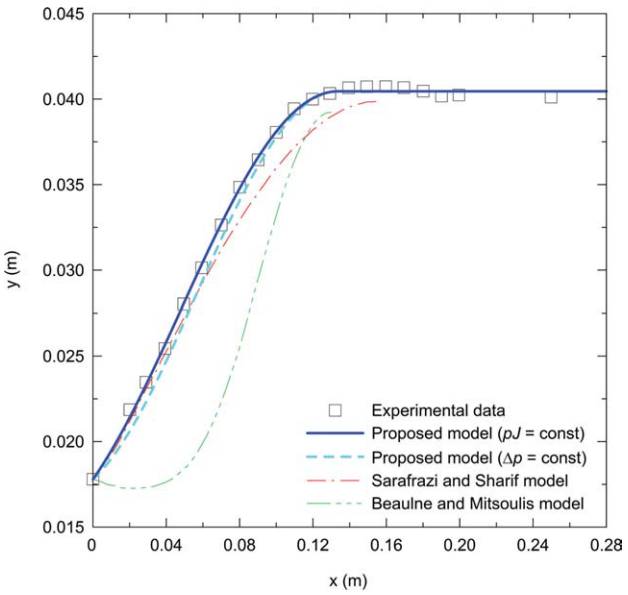

Figure 6 Comparison of the bubble shapes between the proposed model prediction,[30] experiment No. 23 taken from Tas's Ph.D. thesis[18] and the Beaulne/Mitsoulis model prediction[15] and the Sarafrazi/Sharif model prediction.[16] [Color figure can be viewed in the online issue, which is available at wileyonlinelibrary.com.]

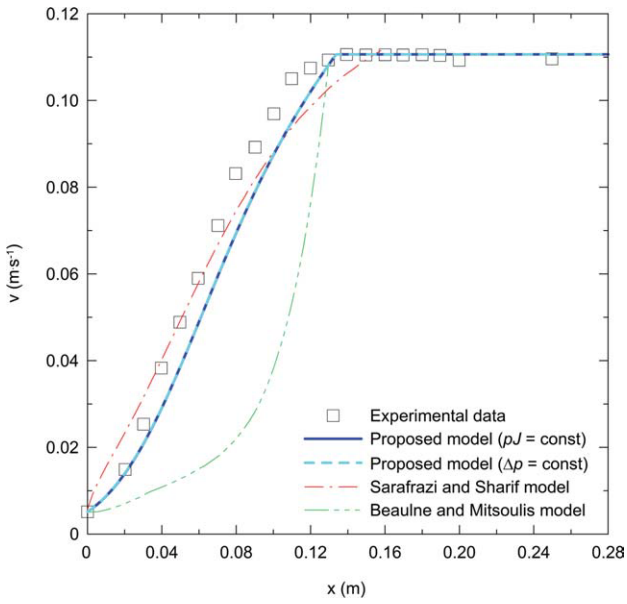

Figure 8 Comparison of the velocity profiles between the proposed model prediction,[30] experiment No. 23 taken from Tas's Ph.D. thesis[18] and the Beaulne/Mitsoulis model prediction[15] and the Sarafrazi/Sharif model prediction.[16] [Color figure can be viewed in the online issue, which is available at wileyonlinelibrary.com.]

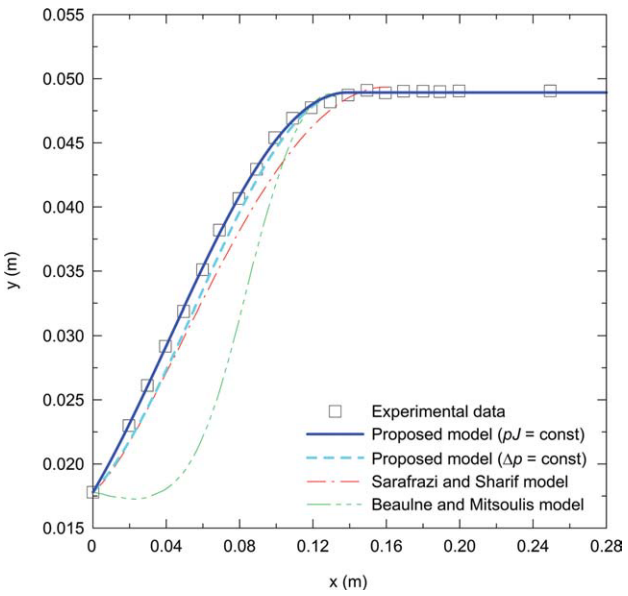

Figure 7 Comparison of the bubble shapes between the proposed model prediction,[30] experiment No. 29 taken from Tas's Ph.D. thesis[18] and the Beaulne/Mitsoulis model prediction[15] and the Sarafrazi/Sharif model prediction.[16] [Color figure can be viewed in the online issue, which is available at wileyonlinelibrary.com.]

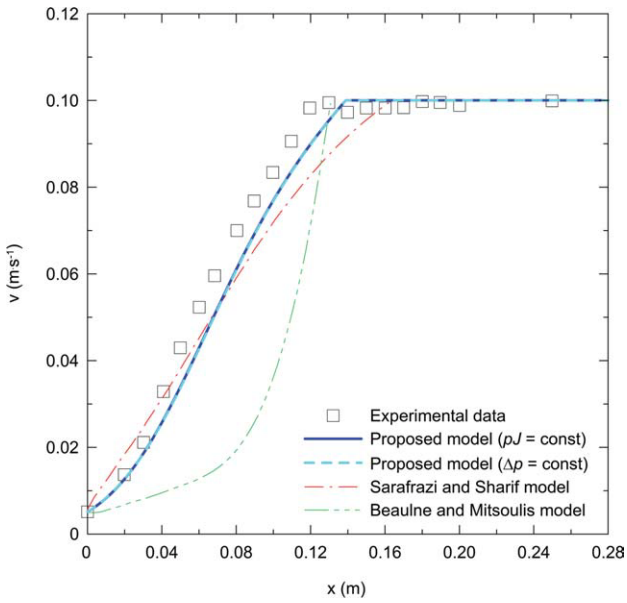

Figure 9 Comparison of the velocity profiles between the proposed model prediction,[30] experiment No. 29 taken from Tas's Ph.D. thesis[18] and the Beaulne/Mitsoulis model prediction[15] and the Sarafrazi/Sharif model prediction.[16] [Color figure can be viewed in the online issue, which is available at wileyonlinelibrary.com.]

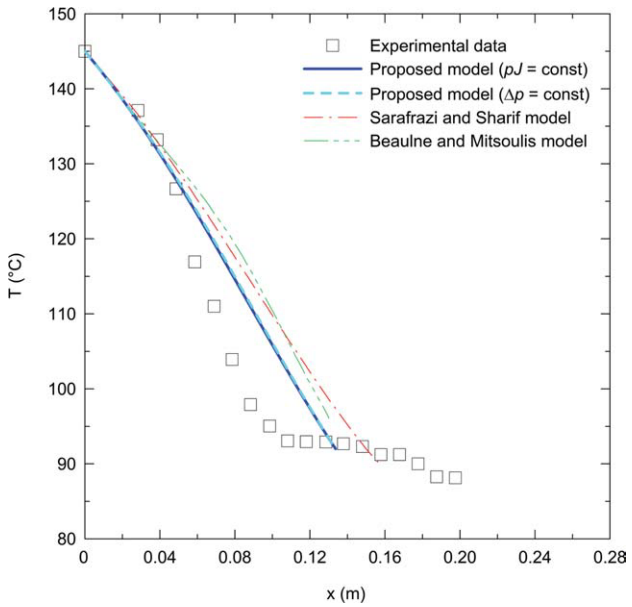

Figure 10 Comparison of the temperature profiles between the proposed model prediction,[30] experiment No. 23 taken from Tas's Ph.D. thesis[18] and the Beaulne/Mitsoulis model prediction[15] and the Sarafrazi/Sharif model prediction.[16] [Color figure can be viewed in the online issue, which is available at wileyonlinelibrary.com.]

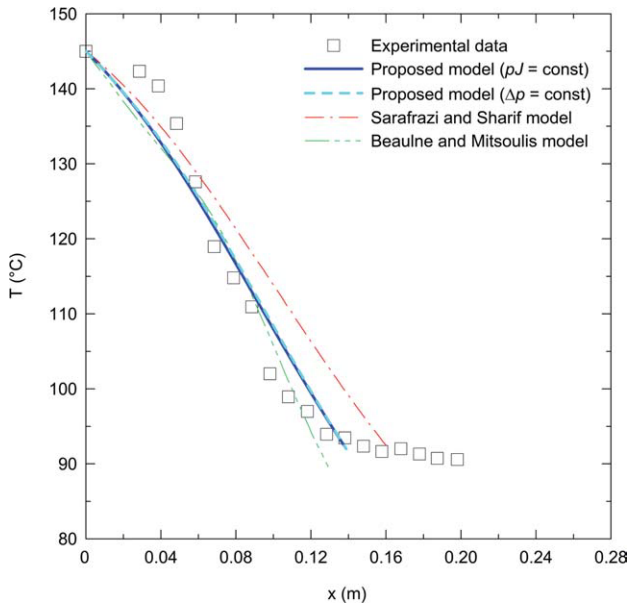

Figure 11 Comparison of the temperature profiles between the proposed model prediction,[30] experiment No. 29 taken from Tas's Ph.D. thesis[18] and the Beaulne/Mitsoulis model prediction[15] and the Sarafrazi/Sharif model prediction.[16] [Color figure can be viewed in the online issue, which is available at wileyonlinelibrary.com.]

mentioned that an additional value of the proposed model is availability of analytical expressions for the freezeline height/heat transfer coefficient, bubble shape, internal bubble pressure and take-up force, which significantly stabilizes numerical scheme and anomalous predictions are avoided.

To the author's knowledge, the effect of biaxial extensional viscosity on the film blowing experiment has not been clearly investigated, yet in the open literature because the measurement of the biaxial extensional viscosity of the polymer melt is very complicated.[42] To fill this gap, the effect of strain hardening level in equibiaxial extensional viscosity (by keeping unchanged shear and uniaxial extensional viscosities) on the film blowing process is investigated here through parameter ψ occurring in eq. (18). In this model, the parameter ψ increase causes the equibiaxial extensional strain hardening decrease for the LDPE L8 as shown in Figure 12 and vice versa. Film blowing modeling of the Tas's experiment No. 23, where parameter ψ was varied

TABLE V
Summarization of Tas's Experimental Data,[18] Zatloukal-Vlcek[a] the Calculated Results for the Fixed Bubble Shape *pJ* and Internal Bubble Pressure Δ*p* are provided in the Parentheses and Without Parentheses, Respectively), Sarafrazi/Sharif [16] and Beaulne/Mitsoulis [15] Model Predictions

Material L8 Models	Experiment 23				Experiment 29			
	Δp (Pa)	F (N)	σ_{11} (MPa)	σ_{33} (MPa)	Δp (Pa)	F (N)	σ_{11} (MPa)	σ_{33} (MPa)
Experimental data (Tas)	85	4.30	0.410	0.068	70	3.50	0.270	0.070
Zatloukal-Vlcek (this work)[a]	85.000 (64.910)	5.895 (5.834)	0.515 (0.510)	0.076 (0.058)	70.000 (46.341)	5.724 (5.619)	0.452 (0.444)	0.083 (0.055)
Sarafrazi and Sharif	69.60	4.80	0.462	0.018	55.84	3.34	0.311	0.038
Beaulne and Mitsoulis	186	1.86	0.196[b]	0.201[b]	168	2.13	0.206[b]	0.245[b]

[a] Zatloukal-Vlcek model considering nonisothermal conditions and non-Newtonian fluid behavior in this work.
[b] σ_{11}, σ_{33} at the freezeline were calculated by using v_d, R_0, H_0, F, Δp, BUR, v_f provided in[15] and Pearson and Petrie equations $\sigma_{11} = \frac{F}{2\pi R_0 \mathrm{BURH}_1}$ and $\sigma_{33} = \frac{R_0 \mathrm{BUR}\Delta p}{H_1}$.

TABLE VI
Summarization of the Proposed Film Blowing Model Predictions for Tas's LDPEs and Processing Conditions

	pJ (m)	v_d (m s^{-1})	v_f (m s^{-1})	$\dot{Q}$ (10^{-7} m^3 s^{-1})	H_1 (10^{-5} m)	J (Pa^{-1})
Exp. 23	0.028611 (0.027605)	0.005143 (0.005143)	0.110627 (0.110627)	12.656 (12.656)	4.5007 (4.5008)	0.001763 (0.002183)
Exp. 29	0.032311 (0.029818)	0.005143 (0.005143)	0.100008 (0.100008)	12.656 (12.656)	4.1161 (4.1163)	0.002076 (0.002812)
	HTC (W m^{-2} K^{-1})	η (Pa s)	$\bar{\eta}$ (Pa s)	a_{TS} (−)	$\overline{a_T}$ (−)	A (−)
Exp. 23	52.53 (51.47)	3,494.6 (3,482.0)	72,273.48 (72,657.1)	20.68 (20.87)	16.40 (16.40)	−0.91280 (−0.76304)
Exp. 29	43.43 (42.20)	3,637.9 (3,626.0)	73,425.8 (74,171.0)	20.18 (20.46)	16.40 (16.40)	−0.87342 (−0.62896)
	$\overline{\dot{\varepsilon}_1}$ (s^{-1})	$\overline{\dot{\varepsilon}_2}$ (s^{-1})	$\overline{\dot{\varepsilon}_3}$ (s^{-1})	$\overline{I_D}$ (s^{-1})	$\overline{II_D}$ (s^{-2})	$\overline{III_D}$ (s^{-3})
Exp. 23	0.82771 (0.82768)	−2.39027 (−2.45498)	1.56257 (1.62730)	4.78055 (4.90996)	4.20479 (4.32668)	−3.09145 (−3.30656)
Exp. 29	0.72051 (0.72046)	−2.13999 (−2.24335)	1.41949 (1.52289)	4.27999 (4.48671)	3.77191 (3.96759)	−2.18868 (−2.46137)

The calculated results for the fixed bubble shape pJ and internal bubble pressure Δp are provided in the parentheses and without parentheses, respectively.

from 0 up to 30, reveals that ψ increase leads to more neck-in like behavior of the bubble and reduction of take-up force (see Figs. 13 and 14, Δp = const.), as well as to reduction of the internal bubble pressure if the bubble shape is fixed (see Fig. 15, pJ = const.). The obtained results clearly show that the role of the biaxial extensional viscosity in the film blowing process is significant. This suggests that the film blowing model predictions might be rather erroneous for the cases when the equibiaxial extensional viscosity is not correctly taken into account by the utilized constitutive equation.

CONCLUSIONS

In this work film blowing process has been model by using variational principles considering minimum energy approach, nonisothermal processing conditions and novel generalized Newtonian model taking steady shear and extensional viscosity of the polymer melts properly into account. The obtained theoretical predictions have been compared with the corresponding experimental data (internal bubble pressure, take-up force, bubble shape, velocity, and temperature profiles) as well as with theoretical predictions of two different Pearson and Petrie based models. It has been

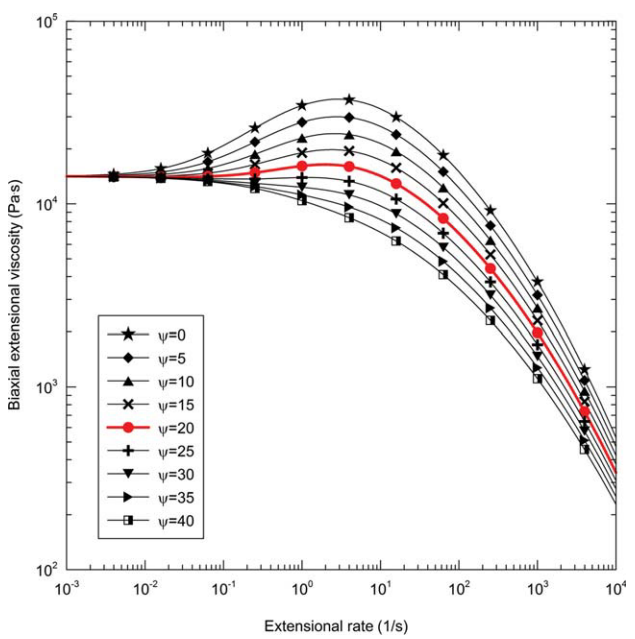

Figure 12 The effect of ψ parameter in the utilized generalized Newtonian model[39] on the biaxial extensional viscosity for LDPE L8. [Color figure can be viewed in the online issue, which is available at wileyonlinelibrary.com.]

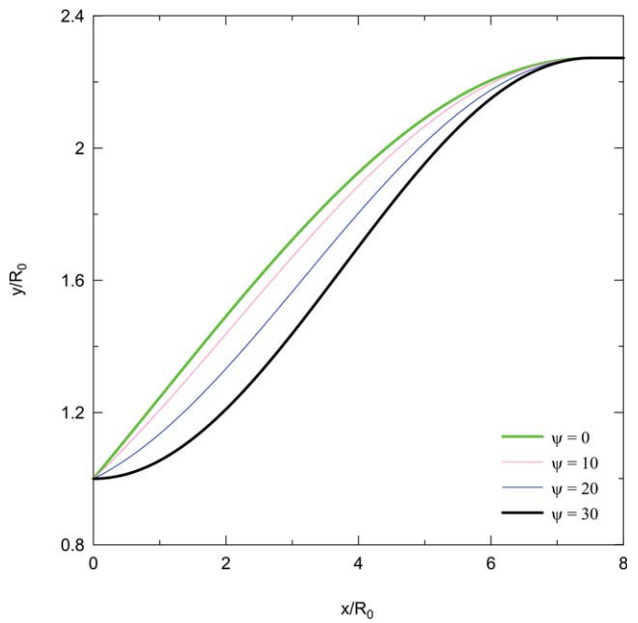

Figure 13 The effect of ψ parameter in the utilized generalized Newtonian model[39] on the bubble shape for experiment No. 23 in Tas's Ph.D. thesis[18] for the fixed Δp. [Color figure can be viewed in the online issue, which is available at wileyonlinelibrary.com.]

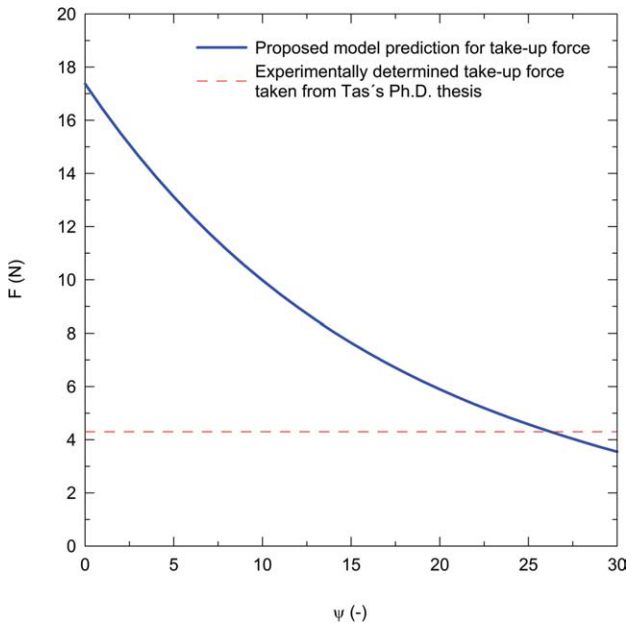

Figure 14 The effect of ψ parameter in the utilized generalized Newtonian model[39] on the predicted take-up force for experiment No. 23 in Tas's Ph.D. thesis[18] for the fixed Δp. [Color figure can be viewed in the online issue, which is available at wileyonlinelibrary.com.]

revealed that both numerical approaches leads to very similar predictions for all investigated variables and the model predictions are in good agreement with corresponding experimental data. The theoretical analysis has revealed that the role of biaxial extensional viscosity on the film blowing process is significant which suggests that film blowing model predictions might be rather erroneous for the cases when the equibiaxial extensional viscosity is not correctly taken into account by the utilized constitutive equation.

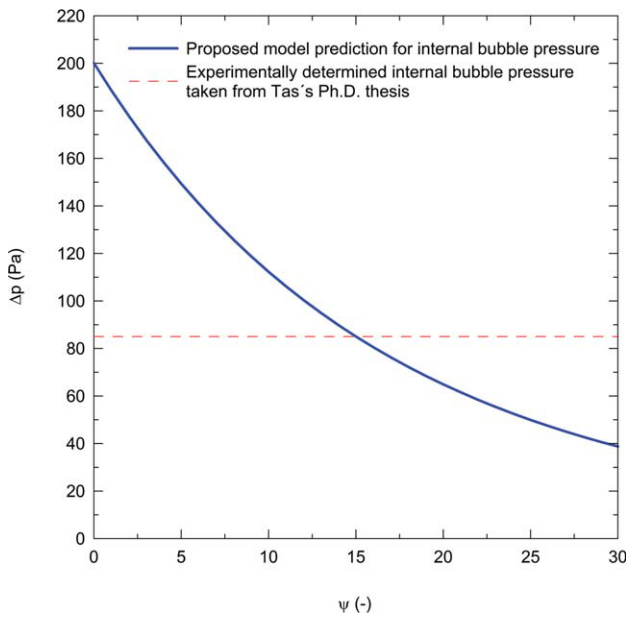

Figure 15 The effect of ψ parameter in the utilized generalized Newtonian model[39] on the predicted internal bubble pressure for experiment No. 23 in Tas's Ph.D. thesis[18] for the fixed bubble shape. [Color figure can be viewed in the online issue, which is available at wileyonlinelibrary.com.]

NOMENCLATURE

A	Zatloukal-Vlcek model function (1)
a	Generalized Newtonian model parameter (1)
a_T	Arrhenius temperature shift factor (1)
$a_{T,\mathrm{Bubble}}$	Bubble temperature shift factor (1)
a_{TS}	Mean value of the Arrhenius temperature shift factor a_T (1)
$\overline{a_T}$	Average temperature shift factor (1)
BUR	Blow-up ratio (1)
C_p	Specific heat capacity (J kg^{-1} K^{-1})
D	Deformation rate tensor (s^{-1})
dx	Element length in x direction (m)
E_a	Activation energy (J mol^{-1})
F, F_{total}, F_N	Take-up force (N)
$F_{\mathrm{thickness}}$	Force acting in the thickness direction of the bubble (N)
G_i	Relaxation modulus in the "i" th relaxation mechanism (Pa)
HTC	Heat transfer coefficient (W m^{-2} K^{-1})
H_0	Bubble thickness at the die exit (m)
H_1	Bubble thickness at the freezeline height (m)
$h(x)$, h	Local film thickness (m)
$\overline{h}$	Mean value of bubble thickness along the bubble (m)
$I_{\lvert D \rvert}$	First invariant of the absolute value of deformation rate tensor (s^{-1})
$\overline{I_{\lvert D \rvert}}$	Mean value of the first invariant of deformation rate tensor (s^{-1})
II_{D}	Second invariant of deformation rate tensor (s^{-2})
$\overline{II_D}$	Mean value of the second invariant of deformation rate tensor (s^{-2})
III_{D}	Third invariants of deformation rate tensor (s^{-3})
$\overline{III_D}$	Mean value of the third invariant of deformation rate tensor (s^{-3})
I	Potential energy functional (N)
J	Bubble compliance $(Pa)^{-1}$
L	Freezeline height (m)
M_n	Number average molecular weight ($g.mol^{-1}$)
M_w	Weight average molecular weight ($g.mol^{-1}$)
M_z	Z average molecular weight (g mol^{-1})
$\dot{m}$	Mass flow rate ($kg.s^{-1}$)
n	Power-law index (1)
p	Internal load (Pa m)
Q	Volumetric flow rate (m^3 s^{-1})
R	Universal gas constant (J $K^{-1}mol^{-1}$)

R_0	Die radius (m)
R_2	Bubble radius at the freezeline height (m)
T	Local bubble temperature (°C)
T_{air}	Air temperature (°C)
T_c	Crystallization temperature (°C)
T_{die}	Die exit melt temperature (°C)
T_r	Reference temperature (°C)
T_s	Average bubble temperature (°C)
T_{solid}	Solidification (freezeline) temperature (°C)
TUR	Take-up ratio 1
V	Bubble volume (m^3)
$v(x)$, v	Local film velocity (m s^{-1})
v_d	Bubble velocity at the die exit (m s^{-1})
v_f	Bubble velocity at the freezeline (m s^{-1})
$\bar{v}$	Mean value of bubble velocity along the bubble (m.s^{-1})
x	Particular distance from the die exit (m)
$y(x)$, y	Local bubble radius (m)

Greek symbols

α	Generalized Newtonian model parameter (s)
α'	Zatloukal-Vlcek model function (1)
β	Generalized Newtonian model parameter (1)
ΔH_f	Heat of crystallization per unit mass (J kg^{-1})
Δp	Internal bubble pressure (Pa)
ε	Phan-Thien-Tanner model parameter (1)
$\dot{\varepsilon}_1$	Extensional rate in machine direction (s^{-1})
$\dot{\varepsilon}_2$	Extensional rate in thickness direction (s^{-1})
$\dot{\varepsilon}_3$	Extensional rate in circumferential direction (s^{-1})
$\bar{\varepsilon}$	Emissivity (1)
$\overline{\dot{\varepsilon}_1}$	Mean value of extensional rate in machine direction (s^{-1})
$\overline{\dot{\varepsilon}_2}$	Mean value of extensional rate in thickness direction (s^{-1})
$\overline{\dot{\varepsilon}_3}$	Mean value of extensional rate in circumferential direction (s^{-1})
ζ	Generalized Newtonian model parameter (1)
η	Viscosity (Pa s)
η_0	Newtonian viscosity (Pa s)
$\overline{\eta}$	Average bubble viscosity (Pa s)
λ	Relaxation time (s)
λ_1	Lagrange multiplier (Pa)
λ_i	Relaxation time in the "i" th relaxation mechanism (s)
ξ	Phan-Thien-Tanner model parameter (1)
π	Ludolf's number (1)
ρ	Polymer density (kg m^{-3})
σ_B	Stefan-Boltzmann constant (W m^{-2} K^{-4})
σ_{11}	Total stress tensor in machine direction (Pa)
σ_{33}	Total stress tensor in circumferential direction (Pa)
τ	Extra stress tensor (Pa)
τ_{11}	Extra stress in the machine directions (Pa)
τ_{22}	Extra stress in the thickness directions (Pa)
ϕ	Average absolute degree of crystallinity (1)
φ	Zatloukal-Vlcek model function (1)
ψ	Generalized Newtonian model parameter (1)
∇v	Velocity gradient tensor (s^{-1})

References

1. Kim, S.; Fang, Y. L.; Lafleur, P. G.; Carreau, P. J. Polym Eng Sci 2004, 44, 283.
2. Mayavaram, R. S. Modeling and simulation of film blowing process," Ph.D. Thesis, A&M University, Texas 2005.
3. Cantor, K. Blown Film Extrusion; Carkl Hanser Verlag: Munich, 2006.
4. Han, C. D.; Park, J. Y. J Appl Polym Sci 1975, 19, 3277.
5. Han, C. D.; Park, J. Y. J Appl Polym Sci 1975, 19, 3291.
6. Yeow, Y. L. J Fluid Mech 1976, 75, 577.
7. Han, C. D.; Shetty, R. Ind Eng Chem Fund 1977, 16, 49.
8. Muke, S.; Connell, H.; Sbarski, I.; Bhattacharya, S. N. J Non-Newtonian Fluid Mech 2003, 116, 113.
9. Minoshima, W.; White, J. L. J Non-Newtonian Fluid Mech 1986, 19, 275.
10. Kanai, T.; White, J. L. Polym Eng Sci 1984, 24, 1185.
11. T. J, Obijeski; Pruitt, K. R. SPE ANTEC Tech Papers 1992, 1, 150.
12. Sweeney, P. A.; Campbell, G. A. SPE ANTEC Tech Papers 1993, 39, 461.
13. Kanai, T.; Campbell, G. A. Film Processing: Progress in Polymer Processing; Hanser Gardner Publications: Munich, 1999.
14. Butler, T. I. SPE ANTEC Tech Papers 2000, 1, 1120.
15. Beaulne, M.; Mitsoulis, E. J Appl Polym Sci 2007, 105, 2098.
16. Sarafrazi, S.; Sharif, F.; Int Polym Process 2008, 23, 30.
17. Muslet, I. A.; Kamal, M. R. J Rheol 2004, 48, 525.
18. Tas, P. P. Film blowing from polymer to product, Ph.D. Thesis, Technische Universiteit Eindhoven, 1994.
19. Gupta, R. K. A new non-isothermal rheological constitutive equation and its application to industrial film blowing, Ph.D. Thesis, University of Delaware, 1981.
20. Pearson, J. R. A.; Petrie, C. J. S. J Fluid Mech 1970, 40, 1.
21. Pearson, J. R. A.; Petrie, C. J. S. J Fluid Mech 1970, 42, 609.
22. Pearson, J. R. A.; Petrie, C. J. S. Plast Polym 1970, 38, 85.
23. Petrie, C. J. S., "Film blowing, blow moulding and thermoforming," in Computational Analysis of Polymer Processing, edited by J. R. A. Pearson and S. M. Richardson; Applied Science: London, 1983, pp. 217–241.
24. Han, C. D.; Park, J. Y. J Appl Polym Sci 1975, 19, 3257.

25. Petrie, C. J. S. Am Inst Chem Eng J 1975, 21, 275.
26. Luo, X. L.; Tanner, R. I. Polym Eng Sci 1985, 25, 620.
27. Ashok, B. K.; Campbell, G. A. Int Polym Proc 1992, 7, 240.
28. Alaie, S. M.; Papanastasiou, T. C. Int Polym Proc 1993, 8, 51.
29. André, J. M.; Demay, Y.; Haudin, J. M.; Monasse, B.; Agassant, J. F. Int J Form Proc 1998, 1, 187.
30. Zatloukal, M. J Non-Newtonian Fluid Mech 2003, 113, 209.
31. Zatloukal, M.; Vlcek, J. J Non-Newtonian Fluid Mech 2004, 123, 201.
32. Zatloukal, M.; Vlcek, J.; Saha, P. Annual Technical Conference - ANTEC, Conference Proceedings 2004, 1, 235.
33. Zatloukal, M.; Vlcek, J. Annual Technical Conference - ANTEC, Conference Proceedings 2005, 1, 139.
34. Zatloukal, M.; Vlcek, J. J Non-Newtonian Fluid Mech 2006, 133, 63.
35. Zatloukal, M.; Mavridis, H.; Vlcek, J.; Saha, P. Annual Technical Conference - ANTEC, Conference Proceedings 2006, 2, 825.
36. Zatloukal, M.; Mavridis, H.; Vlcek, J.; Saha, P. Annual Technical Conference - ANTEC, Conference Proceedings 2007, 3, 1571 2007, 3, 1579.
37. Liu, C. C.; Bogue, D. C.; Spruiell, J. E. Int Polym Proc 1995, 10, 226.
38. Liu, C. C.; Bogue, D. C.; Spruiell, J. E. Int Polym Proc 1995, 10, 230.
39. Zatloukal, M. J Non-Newtonian Fluid Mech 2010, 165, 592.
40. Doufas, A. K.; McHugh, A. J., J Rheol 2001, 45, 1085.
41. Phan-Thien, N.; Tanner, R. I. J Non-Newtonian Fluid Mech 1977, 2, 353.
42. Macosko, C. W. Rheology: Principles, Measurements, and Applications; Wiley: New York, 1994.